In vivo and *ex vivo* measurements: noninvasive assessment of alcoholic fatty liver using 1H-MR spectroscopy

Daniel Keese*
Hüdayi Korkusuz*
Frank Huebner
Dmitry Namgaladze
Bahram Raschidi
Thomas J. Vogl

PURPOSE
We aimed to evaluate the ability of 1H-magnetic resonance spectroscopy (1H-MRS) to detect and quantify hepatic fat content *in vivo* and *ex vivo* in an experimental rat model of alcoholic fatty liver using histopathology, biochemistry, and laboratory analyses as reference.

METHODS
Alcoholic fatty liver was induced within 48 hours in 20 Lewis rats; 10 rats served as control. Intrahepatic fat content determined by 1H-MRS was expressed as the percent ratio of the lipid and water peaks and was correlated with intrahepatic fat content determined histologically and biochemically. Liver enzymes were measured in serum.

RESULTS
Fatty liver could be detected *in vivo* as well as *ex vivo* using 1H-MRS, in all 20 animals. Histologic analysis showed a fatty liver in 16 of 20 animals. Histology and 1H-MRS results were highly correlated (*in vivo*, r=0.93, $P = 0.0005$; *ex vivo*, r=0.92, $P = 0.0006$). Also a strong correlation was noted between *in vivo* 1H-MRS measurements and the fat content determined biochemically (r=0.96, $P = 0.0003$). *Ex vivo* results showed a similarly strong correlation between 1H-MRS and biochemistry (r=0.89, $P = 0.0011$).

CONCLUSION
1H-MRS can be carried out in *ex vivo* models, as well as *in vivo*, to detect and quantify intrahepatic fat content in the acute fatty liver.

From the Departments of Diagnostic and Interventional Radiology (D.K. ✉ dan.ke@gmx.com, H.K., F.H., B.R., T.J.V.) and Biochemistry (D.N.), Johannes Wolfgang Goethe University Frankfurt, Frankfurt, Germany.
* These authors contributed equally to this work.

Alongside diabetes mellitus and obesity, high alcohol consumption is one of the most common causes of fatty liver disease. Acute alcohol-induced steatosis represents the first stage of alcoholic liver disease and is defined as the presence of ≥5% of hepatocytes containing fat (1); over time steatosis progresses to alcoholic steatohepatitis, liver fibrosis, and cirrhosis. Biopsy of liver parenchyma with histologic analysis is currently the gold standard in the detection and quantification of fatty liver disease. Semiquantitative histologic assessment of the liver provides information about fat distribution within the hepatic lobules, can distinguish between simple steatosis and steatohepatitis (alcoholic and nonalcoholic), and can identify healthy livers as well as pathologic processes such as viral hepatitis (2). Despite these advantages, liver biopsy is an invasive procedure with risk of morbidity and complications (3). Furthermore, liver biopsy is not practical for monitoring the progression or regression of fatty liver diseases.

Noninvasive imaging techniques offer several advantages over biopsy for diagnosis and staging of fatty liver diseases including the possibility of simultaneously screening for other liver abnormalities. For example, information on lipid metabolism can be obtained using a noninvasive approach, which is especially useful in high-risk patients with insulin resistance or obesity (4). Moreover, preoperative quantitative assessment in drug-induced fatty liver by chemotherapeutic agents (e.g., methotrexate and irinotecan) can positively influence the risks of perioperative morbidity and mortality. A follow-up of intrahepatic fat content also leads to a better control of therapy using chemotherapy in primary or metastatic liver tumors (5). In addition, it is important to obtain an accurate and fast diagnosis prior to liver transplantation. Thus, the transplantation of a liver with cirrhosis or severe steatosis (> 60%) is associated with high risk of primary nonfunctioning of the organ (6). Furthermore, an acute fatty liver is a significant risk factor for postoperative liver failure after transplantation (7). Better regeneration

of the remaining organ has been shown for donors after partial hepatectomy with intrahepatic fat content of ≤ 5% than those livers with a fat content of 5% to 30% (8).

Noninvasive methods for quantification of steatosis have been developed using ultrasonography, computed tomography (CT) or magnetic resonance imaging (MRI). Ultrasonography is widely used to detect hepatic steatosis, but its sensitivity is reduced in patients with small amounts of fatty infiltration. CT is associated with significant radiation exposure, which limits its use (9). MRI provides sensitive and semiquantitative assessment of tissue, but cannot present a precise and absolute metabolite quantification of intrahepatic fat (10). *In vivo* 1H-magnetic resonance spectroscopy (1H-MRS) has been recently shown to be safe and accurate and has been used as the reference standard (11). However, due to varying results, especially regarding the feasibility and reliability of a quantitative evaluation, further investigation is warranted. Although studies have focused on detecting fatty liver in *in vivo* models we could identify no study exploring the possibility of detecting alcohol-induced fatty liver in *ex vivo* models using 1H-MRS.

Here, we focus on the role of 1H-MRS in the detection of the initial stage of alcohol-induced fatty liver *in vivo* and *ex vivo* using histologic and biochemical analyses as the reference standards.

Methods

Animals

This study was approved by the governmental committee and our institutional

Main points

- 1H-MRS is a noninvasive, safe, and quantitative method for detecting fatty liver in the initial stage, as soon as 48 hours after alcohol consumption.

- In addition, it is possible to detect fatty infiltration precisely in *ex-vivo* models using 1H-MRS, which correlates strongly with the gold standard of histology and biochemical measurements.

- 1H-MRS is superior to other imaging techniques such as ultrasonography, CT, and MRI in the accurate quantification of intrahepatic fat content.

- With its accuracy, 1H-MRS has the potential to be an important clinical tool for the diagnosis of alcoholic steatosis diseases at the onset and help the evaluation of liver transplants before transplantation.

animal research review board. In total 30 female Lewis rats (Charles River), aged 6 to 8 weeks, weighing 200 g were used in this study. Animals were kept under standard conditions with a mean temperature of 22°C±2°C, 55%±10% mean relative humidity, and 12 h light/dark cycle. All animals had free access to water and feed. The maximum number of animals per cage was six. Liver samples were initially extracted from 10 animals to obtain biochemical and histologic results for healthy livers.

Ethanol treatment of rats

Following the method of Ratner et al. (12), each rat in the experimental group was twice given a dose of 9.3 g/kg body weight of 50% ethanol within a period of 24 h. The application took place via oral gavage using a 2 mm (diameter) × 75 mm (length) steel buttoned cannula. The dose of ethanol as well as the mode of application had previously been shown to safely introduce acute fatty liver (13).

Measurements

Summary of the experimental procedures is presented in Table 1. To allow paired comparisons all measurements were repeated on 20 animals before and after ethanol exposure; a separate group of 10 rats served as healthy controls. 1H-MRS and laboratory-chemical examination were performed one day before the first ethanol application and one day after the second ethanol application. During *in vivo* 1H-MRS, rats were anesthetized by isoflurane (2.2% isoflurane in air; 1 L/min) fixed in a supine position and allowed to breath freely. Under this ratio of anesthetic and oxygen, artifacts caused by fast heartbeat and respiratory motions were minimized. For serologic analysis the retrobulbar venous plexus of all animals was punctured and 3 mL blood was withdrawn, following *in vivo* 1H-MRS scans. Serologic levels of aspartate aminotransferase (AST) and alanine aminotransferase (ALT) were determined at the laboratory of the university hospital within 24 h of sample withdrawal. After *in vivo* post-ethanol measurements, the liver was removed and put into a 10 mL syringe plunger. To ensure repeatability, all biochemical and histologic analysis and spectroscopic *ex vivo* measurements were made on the same day.

Magnetic resonance imaging

MRI was performed on a 3.0 T/70 cm horizontal open bore unit (Magnetom Trio,

Siemens Healthcare) with a peak gradient amplitude of 45 mT/m and a maximum slew rate of 200mT/m/ms. An eight-channel multifunctional coil (Clothespin coil; CPC) consisting of two coil pairs of four channel arrays each (Noras MRI products) was used.

For diagnostic imaging of the liver a three-dimensional T1-weighted sequence ("fl3d_vibe") was used with the following parameters: TR, 10.7 ms; TE, 2.75 ms (in-phase, IP) and 6.125 ms (out-of-phase, OP); flip angle, 9°; signal averages, 20; field of view (FOV), 100 mm; slice thickness, 1 mm. Localizing sequences served as the basis for correct placement of the volume of interest (VOI), followed by T1-weighted sequences in the transverse (turbo spin echo: TR, 684 ms; TE, 20 ms) and coronal (turbo spin echo: TR, 745 ms; TE, 20 ms) plane, as well as a T2-weighted sequence in the transverse plane (turbo spin echo; TR, 4820 ms; TE, 79 ms) (Fig. 1).

1H-magnetic resonance spectroscopy

Gradient determination and automatic shimming (applied and controlled by interactive shimming) were applied prior to spectroscopic measurements being taken. For each animal, a single voxel of 10×10×10 mm was placed in the liver, avoiding inclusion of the diaphragm, edges of the liver and vascular and biliary structures (Fig. 2). To achieve precise adjustment of the VOI (i.e., isomorphic to anatomical structures) a VOI-size was selected that would minimize location failures and artifacts, but maximize homogeneity of the liver parenchyma.

1H-MRS data were acquired on the same scanner used for the imaging but including a PRESS (point resolved spectroscopy) sequence with 1500 ms TR and 30 ms TE. Spectral data were acquired in 1024 data points with a 1000 Hz bandwidth, no water suppression, 256 signal averages and a total acquisition time of 6.5 min. Although a longer TR time would minimize T1 effects, the chosen TR time was an acceptable compromise between the T1 effects and the examination time (14). Immediately following 1H-MRS data acquisition, the T2 relaxation times for water and fat were determined with a series of six spectra with TE times of 30 ms, 40, 60, 80, 100, and 120 ms. The complete length of the MRI, including MRI scans (as described above) and 1H-MRS (positioning of the voxel, shimming procedures), did not exceed 40 min.
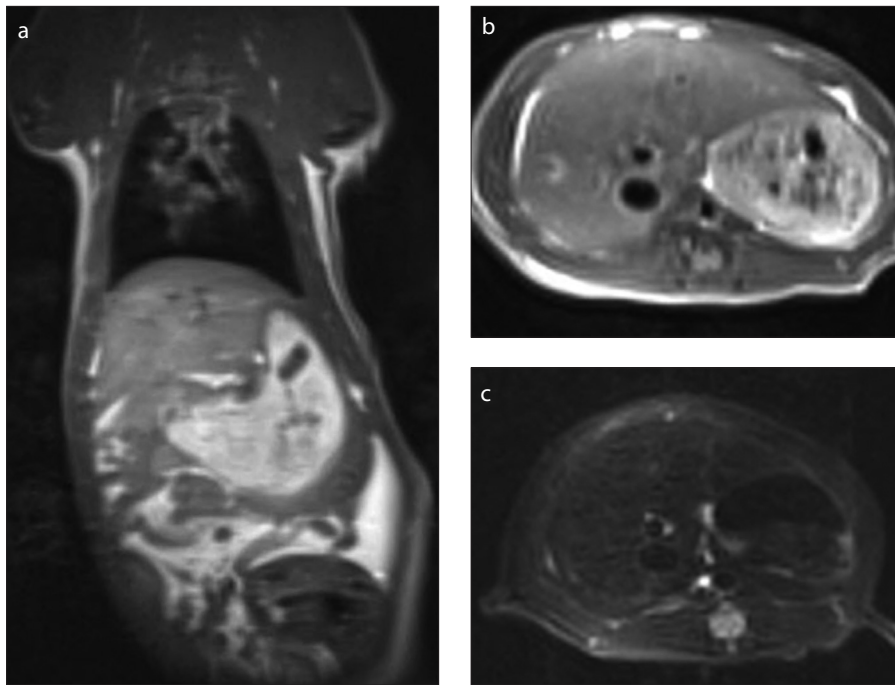
Figure 1. a–c. Coronal T1-weighted **(a)** (TR=745 ms, TE=20 ms), transverse T1-weighted **(b)** (TR=648 ms, TE=20 ms), and transverse T2-weighted **(c)** images *in vivo* (TR=4820 ms, TE=79 ms).
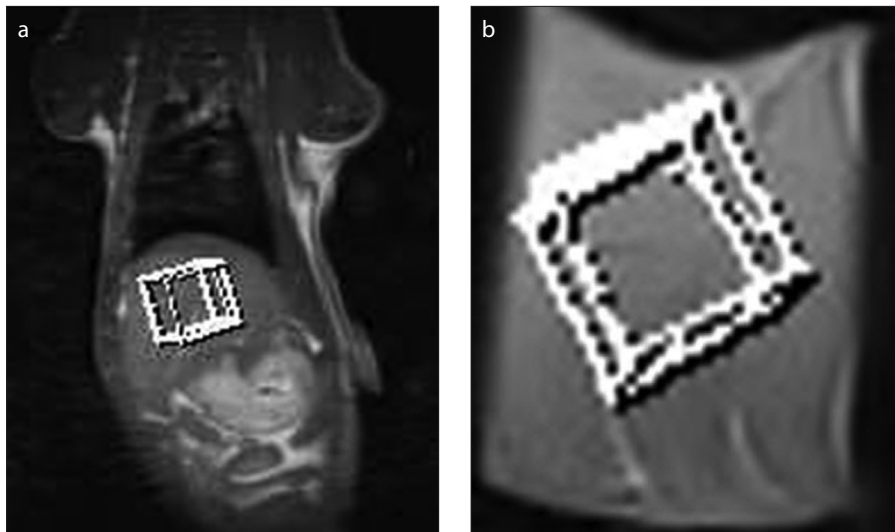
Figure 2. a, b. Coronal T1-weighted image **(a)** *in vivo* illustrating the position of the VOI of 10×10×10 mm and representative coronal T1-weighted image **(b)** illustrating the position of the VOI of 10×10×10 mm *ex vivo*.

All spectra were processed using the standard Siemens software. Postprocessing and quantification included zero filling from 1024 to 2048 data points, multiplication by noise filtering and phase correction, signal fitting of the peaks within the acquired spectra, and integration to find the area under each spectral peak of interest (water at 4.7 ppm, methylene fat at 1.3 ppm). Peak integrations were found by fitting Gaussian functions and were carried out in the real part of the spectrum. The T2

calculation for fat and water was obtained from the signal intensity measured by the various echo times and was determined by a corresponding exponential equation for fat and water as follows:

fat: $TE_{fat-peak-area} = I_0 \times \exp(-TE/T2_{fat})$
water: $TE_{water-peak-area} = I_0 \times \exp(-TE/T2_{water})$,
where I_0 corresponded to the signal intensity at TE=0 ms.

Subsequently, according to Guiu et al. (15), liver fat content (as a percentage) was calculated as follows:

Hepatic fat fraction $(HFF)_{1H-MRS} = 100 \times A_0\text{-}CH_2 / (A_0\text{-}CH_2 + A_0\text{-}H_2O)$, where $A_0\text{-}CH_2$ and $A_0\text{-}H_2O$ describe the peak integrals of methylene and water peaks respectively. For *ex vivo* measurements the removed liver was measured spectroscopically with the same settings described above. The calculated spectrum displayed water and fat metabolites by their specific position on the x-axis (Fig. 3).
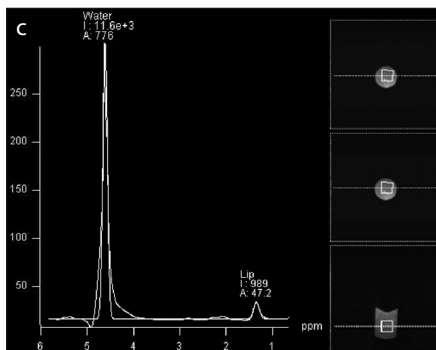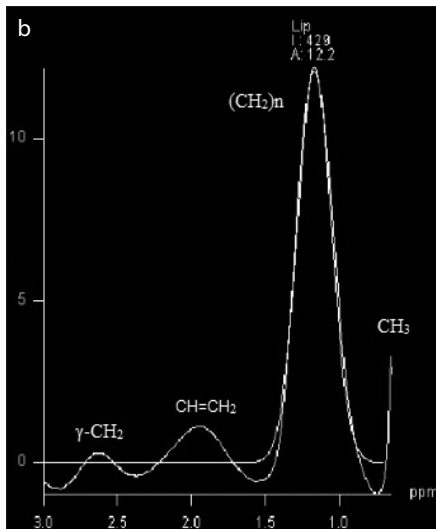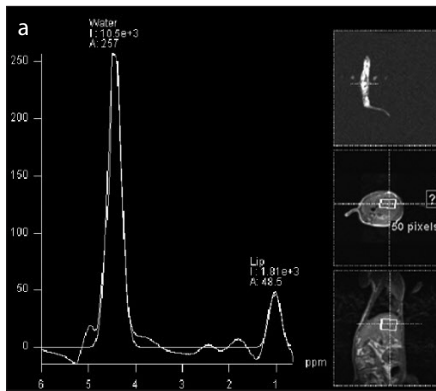
Serologic parameters

For serologic analysis, the retrobulbar venous plexus of all animals was punctured after 1H-MRS measurements, 3 mL blood was extracted and serologic levels of ALT and AST (including the AST/ALT ratio) were determined spectrophotometrically using a Modular P analyzer and a commercial kit (Roche Diagnostics) following IFCC standards.

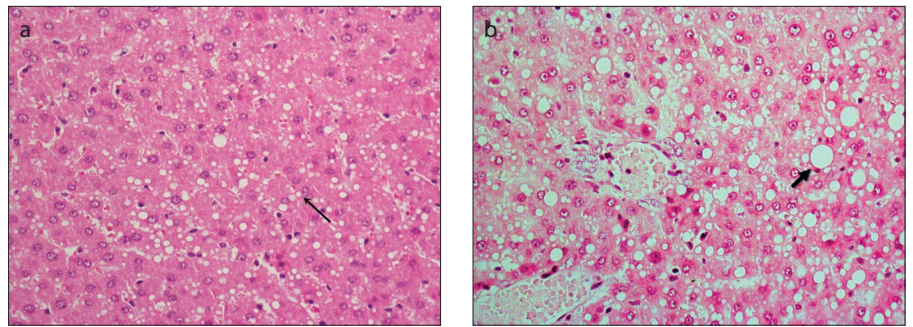### Biochemical analysis/Folch method

Triglyceride content was obtained before and after alcohol intoxication after each 1H-MRS performance and liver extraction was made according to the method of Folch et al. (16). Approximately 100 mg of rat liver tissue samples were homogenized in 2 mL of chloroform-methanol solution (2:1 v/v) followed by centrifugation at 16,000 g for 1 min. The solvent was evaporated in a Speed-Vac concentrator (Thermo Fischer Scientific, Waltham) and the lipid residue resuspended in 100 μL isopropanol. Triglyceride content was determined spectrophotometrically using a Modular P analyzer and a commercial kit from Roche Diagnostics. To minimize unequal distribution of lipids with respect to hepatic triglyceride, several tissue samples were taken from different hepatic regions.

Liver histology

Liver biopsies were fixed in formalin and embedded in paraffin. Liver biopsy sections were analyzed by an experienced hepatopathologist who was blinded to the laboratory parameters and clinical data. The histomorphologic assessment of liver tissue was evaluated by hematoxylin-eosin (HE) staining. The number of fat-containing hepatocytes was estimated semiquantitatively as a percentage (0%–100%), containing macrovesicular fat (fat droplets equal to or larger than the size of the nucleus, often displacing the nucleus) or microvesicular fat (numerous small fat droplets surrounding a centrally located nucleus). For semiquantitative scoring of fatty infiltration, the following values were used: score 0, no visible fat; score 1, <5% of liver surface infil-

Figure 4. a, b. Panel **(a)** shows histologic section of the liver and HE-staining measured 24 hours after the second ethanol intoxication with about 30% fatty degeneration including microvesicular *(thin arrow)* and macrovesicular fat droplets. Panel **(b)** shows approximately 50% mainly macrovesicular fatty degeneration of hepatocytes *(thick arrow)* with leukocyte demarcated single cell necrosis.

Table 1. Summary of experimental procedures

Control group	Procedure
Day 0	• 10 rats anesthetized with isoflurane
	• Explantation of the liver
	• Biochemical determination of TG by Folch method
	• Histologic fat determination
Experimental group	Procedure
Day 1	• 20 rats anesthetized with isoflurane
	• Spectroscopic measurement of hepatic lipid concentration
	• Blood sample (3 mL) taken for determination of AST and ALT
Day 2	• First administration of ethanol
Day 3	• Second administration of ethanol
Day 4	• Same 20 rats (day 1–3) anesthetized with isoflurane
	• Spectroscopic measurement of HFF
	• Blood sample (3 mL) taken for determination of AST and ALT
	• Explantation of the liver
	• Biochemical determination of TG by Folch method
	• Histologic fat determination

TG, triglycerides; AST, aspartate aminotransferase; ALT, alanine aminotransferase; HFF, hepatic fat fraction.

Figure 3. a–c. 1H-MRS spectrum of rat no. 13 of the post-ethanol group *in vivo* **(a)** with a hepatic fat fraction (HFF) of 14.7%. The spectrum shows the dominant water peak at 4.7 ppm with a prominent lipid peak ([CH$_2$]n) at 1.1–1.3 ppm (I, integral; A, amplitude). Panel **(b)** shows enlargement of the lipid peak of rat no. 7; y-axis shows amplitude, x-axis shows the frequency of the corresponding metabolites: (CH$_2$)n, saturated lipids at 1.3 ppm; CH=CH$_2$, unsaturated lipids at 2.0 ppm; CH$_3$, mobile lipids at 0.6 ppm; γ - CH$_2$, glutamate/glutamine at 2.6 ppm. The right side of panel **(a)** shows the sectional plane and the positioning of the voxel in the localizer sequence and in the coronal and transverse planes. Rat no. 9 of the post-ethanol group *ex vivo* in panel **(c)** shows a HFF of 7.9% with dominant water peak and a prominent lipid peak ([CH$_2$]n) at 1.1–1.3 ppm. The right side of panel **(c)** shows the explanted liver in a 10 mL syringe plunger, including the sectional plane.

trated by fat; score 2, 5%–25% fat; score 3, 25%–50% fat; score 4, >50% fat (17) (Fig. 4).

Statistical analysis

Statistical analysis was performed by using BiAS version 8.4 (Epsilon). Agreement between the fat content measured spectroscopically (i.e., HFF) *in vivo* as well as *ex vivo* with histology was assessed in two steps. First, we drew a scatterplot including a regression line and calculated the coefficient of determination (r^2) to assess the relationship between HFF and histology. Second, Spearman's nonparametric correlation coefficient (r) was calculated to determine the correlation between the different diagnostic methods (HFF vs. biochemistry, HFF vs. ALT, and HFF vs. AST).

The Shapiro-Wilk test was used to test the normal distribution of the datasets (ALT, AST, triglyceride-content, HFF data, and T2 times). When variables were normally distributed, results were expressed as mean values and standard deviation (SD), otherwise median and 25%–75% interquartile range (IQR) was reported. Because of the semiquantitative nature of the values, the Shapiro-Wilk test was not applied to histopathologic data. Wilcoxon signed-rank test was used to compare the difference among the various pre- and post-ethanol results of AST, ALT, triglycerides, and HFF and were also given for the T2 times for water and fat protons determined *in vivo* and *ex vivo*. Results were considered to be significant at $P < 0.05$.
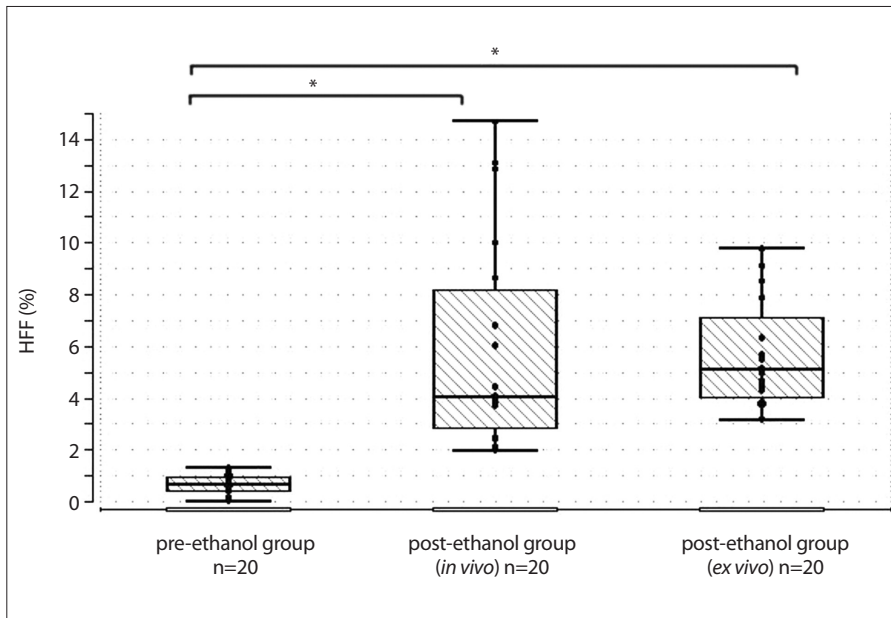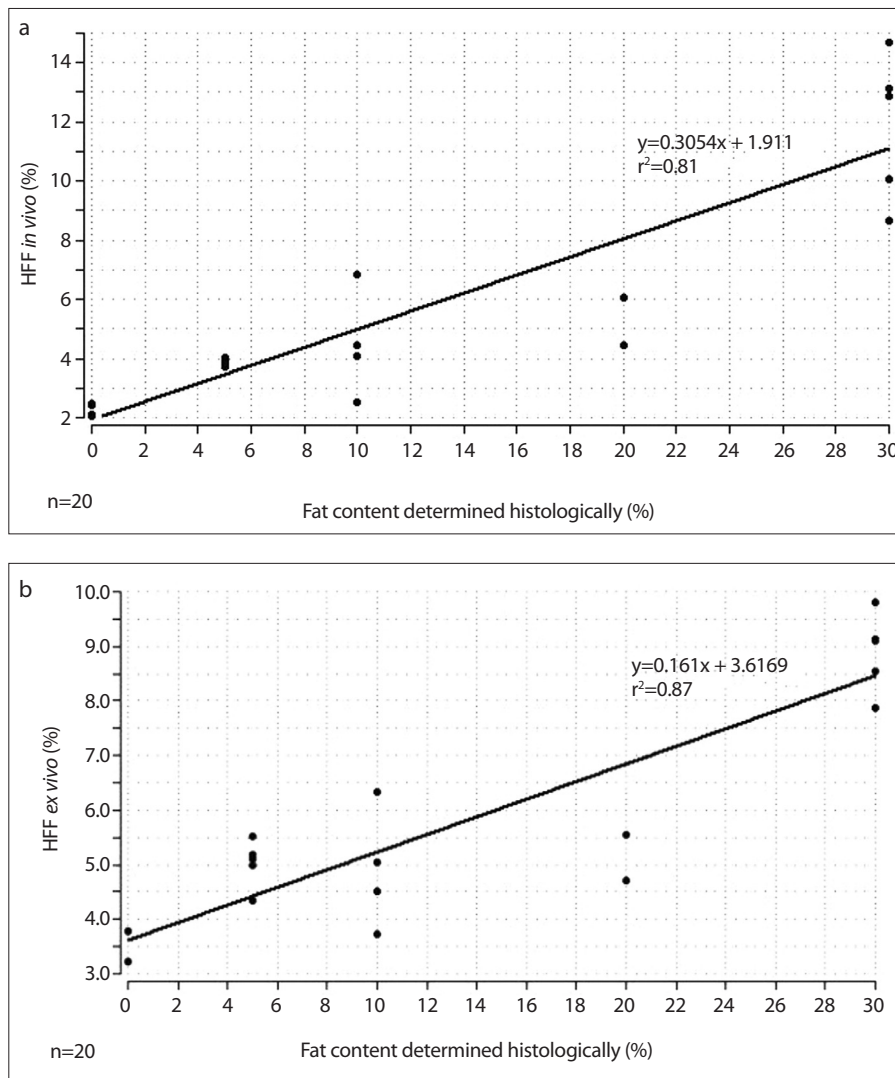
Figure 5. Reproducibility of fat measurements by 1H-MRS (hepatic fat fraction, HFF) obtained from *in vivo* livers before ethanol intoxication (left box plot), after ethanol intoxication (middle box plot), and *ex vivo* livers (right box plot) (n=20, for each group). In the pre-ethanol group mean HFF was 0.69% (SD, ±0.33%; *P* = 0.7483). After ethanol intoxication *in vivo* measurements showed a mean of 5.8% (median of 4.1% (IQR, 2–15 U/l; *P* = 0.002) and for *ex vivo* livers 5.67% (SD, ±2.09%; *P* = 0.0543).
*Significant difference between pre- and post-ethanol HFF measured *in vivo* (*P* = 0.0029), as well as pre- and post-ethanol HFF measured *ex vivo* (*P* < 0.001).

Table 2. Comparison of spectroscopic and histologic hepatic fat content and serologic and biochemical diagnostics after ethanol intoxication

Rat no.	1H-MRS *in vivo* HFF (%)	1H-MRS *ex vivo* HFF (%)	Histology (%)	TG (mg/g)	ALT (U/L)	AST (U/L)
1	6.06	5.56	20	23.81	126	868
2	12.86	9.11	30	37.18	147	897
3	2.03	3.77	0	5.27	67	255
4	3.9	4.70	5	13.85	114	348
5	4.42	5.52	10	16.38	123	465
6	2.11	3.77	0	7.04	72	240
7	2.41	3.21	0	3.85	74	290
8	3.8	5.09	5	10.53	104	323
9	8.66	7.86	30	24.4	146	832
10	3.74	3.73	5	10.7	104	387
11	6.82	6.34	10	23.34	144	761
12	2.51	5.03	10	7.14	79	314
13	14.69	9.81	30	41.1	154	1116
14	4.07	4.51	10	17.81	123	576
15	4.05	4.33	5	12.2	117	546
16	10.04	8.53	30	29.7	146	784
17	13.13	9.14	30	40.81	149	1058
18	4.44	5.18	20	16.62	126	739
19	2.47	3.23	0	8.25	77	323
20	3.89	4.98	5	19.02	106	311

No, number; HFF, hepatic fat fraction; TG, triglyceride; ALT, alanine aminotransferase; AST, aspartate aminotransferase.

Results

Histologically measured mean intrahepatic fat before ethanol intoxication was 1.5%±1.42% (n=10). Liver steatosis (hepatic fat infiltration >5% hepatocyte) after ethanol intoxication was present in 16 of 20 rodents (80%). A histologic grading score of 0 was found in four animals, grade 1 in five animals, grade 2 in six animals, and grade 3 in five animals. The percent mean value of steatosis was 12.75±11.64%.

ALT and AST activity values were determined in all 20 animals of the experimental group before and after ethanol intoxication. The mean ALT was 51.29±13.64 U/L before ethanol intoxication, which increased significantly to 114.9±28.78 U/L after ethanol intoxication (*P* < 0.001). The mean AST value increased significantly from 165.24±63.15 U/L before ethanol intoxication to a median of 571.65 U/L (IQR, 240–1116 U/L) after ethanol intoxication (*P* < 0.001). The AST:ALT ratio (De-Ritis quotient) was >2 in all 20 animals.

Triglyceride content of the liver of healthy rats is typically assumed to be about 4 to 7 mg/g (18), which can increase four-fold within 12 h of ethanol intoxication (19). The triglyceride content before ethanol intoxication showed a mean of 6.78±2.19 mg/g and increased to 18.45±11.51 mg/g at 24 h after the second ethanol dose (*P* < 0.001). Thus, a triglyceride content that corresponded to an acute fatty degeneration of the liver could be determined.

1H-MRS measurements were carried out before the initial administration of ethanol and 24 h after the second ethanol intoxication. Detection of intrahepatic fat (i.e., HFF) was achieved in all 20 animals before and after ethanol intoxication (*in vivo* and *ex vivo*). The mean value of HFF was 0.69%±0.33% before ethanol intoxication. After ethanol intoxication, HFF was measured as a median of 4.1% (IQR, 2%–15%) *in vivo* and as a mean of 5.67%±2.09% *ex vivo* (Fig. 5). Pre- and post-ethanol HFF values were significantly different both *in vivo* (*P* < 0.001) and *ex vivo* (*P* < 0.001).

In vivo post-ethanol mean T2 times were as follows: tissue water protons, 34.1 ms (range, 23.8–47.6 ms); tissue fat protons, 53 ms (range, 38.2–86.2 ms). *Ex vivo* post-ethanol mean T2 times were as follows: tissue water protons, 32.3 ms (range, 24.1–42.3 ms); tissue fat protons, 56.2 ms (range, 42.1–83.4 ms). There was no significant difference between T2 times measured *in vivo* and *ex vivo* (*P* = 0.821 for water protons; *P* = 0.7936 for fat-protons).

Figure 6. a, b. Plot of calculated linear dependency of histology vs. HFF *in vivo* (**a**) is shown with the regression line: y=0.3054x + 1.911; r²=0.81, P < 0.001; n=20. A similar plot for histology vs. HFF *ex vivo* (**b**) is shown with the regression line: y=0.161x + 3.6169; r²=0.87, P < 0.001; n=20.

Table 3. Spearman correlation coefficient (r) describing the relationship between different diagnostic methods

Diagnostic method	Histology	Folch	AST	ALT
1H-MRS (HFF) *in vivo*	0.93	0.96	0.96	0.82
1H-MRS (HFF) *ex vivo*	0.92	0.89	0.95	0.90
1H-MRS, 1H-magnetic resonance spectroscopy; HFF, hepatic fat fraction; AST, aspartate aminotransferase; ALT, alanine aminotransferase.				

Spectroscopically measured HFF was compared with the laboratory-determined chemical parameters of AST and ALT. *In vivo* spectroscopically measured HFF of alcohol-toxic fatty livers correlated positively with AST (r=0.96, P < 0.001) and ALT (r=0.95, P < 0.001). Similarly, *ex vivo* post-ethanol values showed a strong correlation between 1H-MRS and the serologic parameters AST (r=0.82, P < 0.001) and ALT (r=0.9, P < 0.001). Furthermore, histologic results (as the percentage of infiltrated fat hepatocytes) were compared with spectroscopically measured lipid content. Although the spectroscopic values were lower in direct comparison of histology and 1H-MRS, a significant positive correlation was found between the two methods (*in vivo*, r=0.93, P = 0.0005; *ex vivo*, r=0.92, P < 0.001) (Fig. 6).

A high correlation was also discovered between 1H-MRS and biochemically determined *in vivo* and *ex vivo* fat content (*in vivo*, r=0.96, P < 0.001; *ex vivo*, r=0.89, P = 0.0011). Comparison between HFF *in vivo* and HFF *ex vivo* showed no significant difference between the mean values of both groups (P = 0.7623). Table 2 shows a summary of all values of the experimental group after ethanol intoxication. Summary of all r values is reported in Table 3.

Discussion

The assessment of liver fat infiltration is typically based on liver biopsy with subsequent histologic analysis, which is considered as the diagnostic gold standard. However, liver biopsy is an invasive procedure that is associated with complications and sampling errors. Several studies have shown that the use of 1H-MRS is an established noninvasive method to detect and quantify fat content in human liver steatosis (20). As a quantitative method, 1H-MRS has a unique advantage over ultrasonography, CT, and MRI (which are qualitative or semi-quantitative) (21). In recent years various strategies have been developed to obtain volume-selective 1H-MRI spectra from liver parenchyma *in vivo* and to enhance this technique; however, no study has been conducted that explores the possibility of using 1H-MRS to detect an acute alcohol-induced fatty liver in animal models *ex vivo*.

Here, we successfully detected a lipid signal by a spectroscopic approach in all animals before and after ethanol intoxication, including animals in which no fatty degeneration of hepatocytes was observed histologically. The presence of histologically detectable steatosis was found in only 80% of biopsies after ethanol intoxication. In addition, the results demonstrated a discrepancy between the HFF measured spectroscopically and the histologic fat determination. For example, rat no. 9 showed a fatty degeneration of about 30% by a histologic approach, compared to a value of approximately 9% by 1H-MRS *in vivo*. This result suggests that patients are likely to be ranked higher by histologic grading compared with spectroscopic measurements. One possible explanation for this discrepancy is the semiquantitative nature of histologic classification of obesity, which relies on recording the percentage of hepatocytes within the microscopic view that display visible steatosis. Consequently, the visual estimate and evaluation of only

a

b
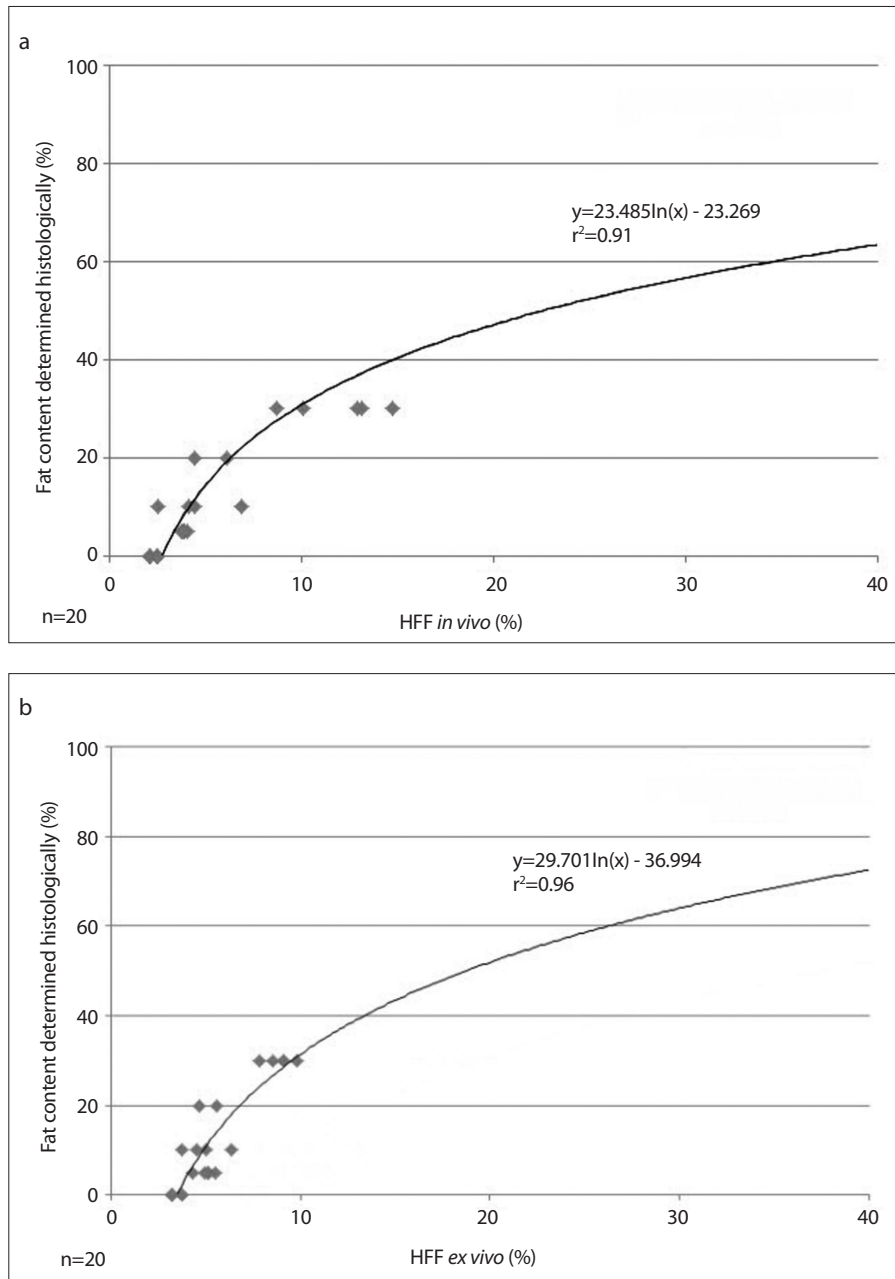
Figure 7. a, b. Calibration graph with exponential dependency of histology vs. HFF *in vivo* (**a**): y=23.485 ln(x) - 23.269; r^2=0.91, *P* < 0.001; n=20. The calibration graph with exponential dependency of histology vs. HFF *ex vivo* (**b**): y=29.701 ln(x) - 36.994; r^2=0.96, *P* < 0.001; n=20.

a small liver biopsy leads to sampling errors and inaccurate measurements. Ratziu et al. (22) found that there is a correspondence of only ~60% between two liver biopsies of the same patient. In addition, variability in the severity of steatosis by histologic examination within a single biopsy sample has been reported (23). Moreover the heterogeneity of distribution and quantity of fatty hepatocytes in liver biopsies can lead to distorted and false negative results, especially in low-grade fatty degeneration (24).

The present discrepancy between histology and 1H-MRS results support not only

a linear dependence but also the use of a calibration graph. In this case, nonlinear exponential fit is performed based on the collected data and four-step grading of the histologic measurement is performed with the assumption that the curve starts at a histologic fat content of 0% (Fig. 7). Consequently, there is an even higher r^2 value than with the linear dependence approach (*in vivo*, r^2=0.91; *ex vivo*, r^2=0.96). Different results in the comparison of intrahepatic fat content measured histologically and spectroscopically have also been reported in other studies. d'Assignies et al. (25) report-

ed a histologic fat content of 47.5%±19.6% in 20 patients with steatosis, which dropped to 18.1%±9% when assessed by 1H-MRS. The calculated correction coefficient for adjusting the 1H-MRS measurements on the histologic fat content was 2.6. Also, Hájek et al. (26) used linear and nonlinear models to describe the relationship between 1H-MRS and histology. The correction coefficients of the linear models for three groups of 77 patients were 3.3, 4.2, and 6.1. In the present work, correction coefficients were calculated as 2.2 and 2.5 for *in vivo* and *ex vivo* measurements, respectively. The clinical relevance of the differences between the findings of histologic and spectroscopic approaches is currently under discussion (27). There remains no consensus on a standardized normal value for spectroscopically measured intrahepatic fat. An initial proposal suggested a value of 20% as a reference threshold (28). A subsequent study has suggested that >3.6% intrahepatic fat measured by 1H-MRS should be considered as steatosis (29). In the present study, a HFF of 3.7% measured by 1H-MRS corresponded to a histologically determined fatty liver (involvement of >5% of hepatocytes by histologic analysis).

For the exact determination of HFF, the spectroscopic peak areas should be corrected for T2 relaxations as described above. In a series of studies, the following average T2 values were calculated by the 3.0 T MRI system: T2 water, 27 ms (range, 12.4–54.3 ms) and T2 fat, 61 ms (range, 28–82.2 ms) (30); T2 water, 12.4–54.3 ms and T2 fat, 49–60 ms (26); T2 water, 28 ms (range, 22–42 ms) and T2 fat, 64 ms (range, 36–99 ms) (31). These values are consistent with the results obtained in the present study.

The additional comparison of the 1H-MRS data with the biochemical analysis of extracted tissue samples is a unique advantage of our study. The high correlation of 1H-MRS and triglyceride content (r=0.96, *in vivo*; r=0.89, *ex vivo*) suggests the reproducibility of the spectroscopic analysis to other quantification methods and confirm the results of the correlation between histology and 1H-MRS. Although triglyceride levels were too low for the formation of macroscopic vesicles that could be detected histologically, these could be measured using the Folch method. In conjunction with the sufficient sensitivity of 1H-MRS for the quantification of HFF, the results of the biochemical analysis showed similarly strong correlation with the spectroscopic data compared with histologic fat content determination.

The significant correlation between 1H-MRS and the liver enzyme activity data confirm the hypothesis that 1H-MRS may be able to predict the function and condition of diseased livers. Reasons for elevated serum aminotransferase activities include alcohol abuse, medication, autoimmune hepatitis, hepatic steatosis, and nonalcoholic steatohepatitis (32). Compared with ALT, AST activity has been reported to be more sensitive to liver damage caused by alcohol (33), which would explain the slightly better correlation between *in vivo* 1H-MRS results and AST activity in our analyses. The AST/ALT ratio has been used to distinguish cirrhotic from noncirrhotic patients and patients with nonalcoholic liver disease from those with alcoholic liver disease (34). However, it should be noted that liver enzyme data alone can only provide a general indication of liver function. More precise staging of acute decompensation can be given only in conjunction with other laboratory tests or with the De-Ritis quotient.

The results of this work indicate that *ex vivo* 1H-MRS measurements work especially well. The comparisons between *ex vivo* 1H-MRS and biochemical triglycerides determination, as well as the histologic analyses show a similarly strong correlation to *in vivo* measurements. These data suggest that 1H-MRS is a useful method for the detection of fat content, especially from liver grafts of deceased donors before liver transplantation.

The measured range of fat values in *ex vivo* measurements showed less variation than *in vivo* measurements, which might be accounted for in three ways. First, during *in vivo* measurements perfusion of the liver is affected by the blood pressure and blood flow, which is not purely steady state, whereby in *ex vivo* the blood-influence is missing. Thus, measurements of fatty infiltration in *ex vivo* livers are likely to be more accurate. Second, respiratory motion in living rodents can lead to erroneous fat signal contamination of the 1H-MRS spectra. Third, a different fat-water ratio could be crucial for higher fat values in most of the *ex vivo* livers. T2-weighted images receive their contrast from the transverse magnetic relaxation of water protons in tissue. A loss of water due to the explantation of the liver may be an important cause of a lower water signal and subsequent higher fat content values. Additionally, systematic variations in the two methods (e.g., spatial volume effects in *in vivo* 1H-MRS, shrinkage artifacts) may adversely affect different results.

Our study has some limitations. It should be noted that 1H-MRS measurements were carried out under highly standardized experimental conditions. Nevertheless, motion of the animals, the small voxel size and the difficulty of obtaining field homogeneity in a small object using a full body scanner lead to inhomogeneities that partially extend and distort the spectral lines. Free breathing of the rats is a principal cause of artifacts during 1H-MRS measurements. In addition, different technical conditions such as magnetic field strength, localization methods, or different repetition times may influence the spectroscopic results. Another limitation of this study is the small number of animals. In order to substantiate the results in the present study, the *ex vivo* data should be validated and confirmed by further research.

In conclusion, our findings suggest 1H-MRS as a noninvasive, safe, and accurate quantitative method for detecting acute fatty liver, as soon as 48 h after alcohol consumption. Furthermore, 1H-MRS shows the potential to detect fatty infiltration especially in *ex vivo* models. With its increasing accuracy 1H-MRS is likely to become an important clinical tool, potentially becoming the technique of choice for the diagnosis of early-stage alcoholic liver diseases, as well as for analyzing and evaluating liver transplants before transplantation.

Conflict of interest disclosure
The authors declared no conflicts of interest.

References
1. Reddy JK, Rao MS. Lipid metabolism and liver inflammation. II. Fatty liver disease and fatty acid oxidation. Am J Physiol Gastrointest Liver Physiol 2006; 290:G852–858. [CrossRef]
2. Hubscher SG. Histological assessment of non-alcoholic fatty liver disease. Histopathology 2006; 49:450–465. [CrossRef]
3. Smith EH. Complications of percutaneous abdominal fine-needle biopsy. Review. Radiology 1991; 178:253–258. [CrossRef]
4. Thomas EL, Hamilton G, Patel N, et al. Hepatic triglyceride content and its relation to body adiposity: a magnetic resonance imaging and proton magnetic resonance spectroscopy study. Gut 2005; 54:122–127. [CrossRef]
5. McCormack L, Petrowsky H, Jochum W, Furrer K, Clavien PA. Hepatic steatosis is a risk factor for postoperative complications after major hepatectomy - A matched case-control study. Ann Surg 2007; 245:923–930. [CrossRef]
6. Selzner M, Clavien PA. Fatty liver in liver transplantation and surgery. Semin Liver Dis 2001; 21:105–113. [CrossRef]
7. Todo S, Demetris AJ, Makowka L, et al. Primary nonfunction of hepatic allografts with preexisting fatty infiltration. Transplantation 1989; 47:903–905. [CrossRef]
8. Ma X, Holalkere NS, Kambadakone RA, Mino-Kenudson M, Hahn PF, Sahani DV. Imaging-based quantification of hepatic fat: methods and clinical applications. Radiographics 2009; 29:1253–1277. [CrossRef]
9. Saadeh S, Younossi ZM, Remer EM, et al. The utility of radiological imaging in nonalcoholic fatty liver disease. Gastroenterology 2002; 123:745–750. [CrossRef]
10. Hatta T, Fujinaga Y, Kadoya M, et al. Accurate and simple method for quantification of hepatic fat content using magnetic resonance imaging: a prospective study in biopsy-proven nonalcoholic fatty liver disease. J Gastroenterol 2010; 45:1263–1271. [CrossRef]
11. Chalasani N, Younossi Z, Lavine JE, et al. The diagnosis and management of non-alcoholic fatty liver disease: Practice guideline by the American Association for the Study of Liver Diseases, American College of Gastroenterology, and the American Gastroenterological Association. Am J Gastroenterol 2012; 107:811–826. [CrossRef]
12. Ratner AV, Carter EA, Pohost GM, Wands JR. Nuclear magnetic resonance spectroscopy and imaging in the study of experimental liver diseases. Alcohol Clin Exp Res 1986; 10:241–245. [CrossRef]
13. Reboucas G, Isselbacher KJ. Studies on the pathogenesis of the ethanol-induced fatty liver. I. Synthesis and oxidation of fatty acids by the liver. J Clin Invest 1961; 40:1355–1362. [CrossRef]
14. Orlacchio A, Bolacchi F, Cadioli M, et al. Evaluation of the severity of chronic hepatitis C with 3-T1H-MR spectroscopy. AJR Am J Roentgenol 2008; 190:1331–1339. [CrossRef]
15. Guiu B, Petit JM, Loffroy R, et al. Quantification of liver fat content: comparison of triple-echo chemical shift gradient-echo imaging and in vivo proton MR spectroscopy. Radiology 2009; 250:95–102. [CrossRef]
16. Folch J, Lees M, Sloane Stanley GH. A simple method for the isolation and purification of total lipids from animal tissues. J Biol Chem 1957; 226:497–509.
17. Brunt EM. Nonalcoholic steatohepatitis: definition and pathology. Semin Liver Dis 2001; 21:3–16. [CrossRef]
18. Theuer RC, Martin WH, Friday TJ, Zoumas BL, Sarett HP. Regression of alcoholic fatty liver in the rat by medium-chain triglycerides. Am J Clin Nutr 1972; 25:175–181.
19. Bode C, Kono H, Goebell H, Martini GA. Zur Pathogenese der Fetteinlagerung in die Leber durch Alkohol. Klin Wochenschr 1970; 19:1180–1188. [CrossRef]
20. Bohte AE, van Werven JR, Bipat S, Stoker J. The diagnostic accuracy of US, CT, MRI and 1H-MRS for the evaluation of hepatic steatosis compared with liver biopsy: a meta-analysis. Eur Radiol 2011; 21:87–97. [CrossRef]
21. Mehta SR, Louise Thomas E, Patel N, et al. Proton magnetic resonance spectroscopy and ultrasound for hepatic fat quantification. Hepatol Res 2010; 40:399–406. [CrossRef]
22. Ratziu V, Charlotte F, Heurtier A, et al. Sampling variability of liver biopsy in nonalcoholic fatty liver disease. Gastroenterology 2005; 128:1898–1906. [CrossRef]
23. Turlin B, Ramm GA, Purdie DM, et al. Assessment of hepatic steatosis: comparison of quantitative and semiquantitative methods in 108 liver biopsies. Liver Int 2009; 29:530–535. [CrossRef]

24. Mennesson N, Dumortier J, Hervieu V, et al. Liver steatosis quantification using magnetic resonance imaging: a prospective comparative study with liver biopsy. J Comput Assist Tomogr 2009; 33:672–677. [CrossRef]

25. d'Assignies G, Ruel M, Khiat A, et al. Noninvasive quantitation of human liver steatosis using magnetic resonance and bioassay methods. Eur Radiol 2009; 19:2033–2040. [CrossRef]

26. Hajek M, Dezortova M, Wagnerova D, et al. MR spectroscopy as a tool for in vivo determination of steatosis in liver transplant recipients. MAGMA 2011; 24:297–304. [CrossRef]

27. Noworolski SM, Lam MM, Merriman RB, Ferrell L, Qayyum A. Liver steatosis: concordance of MR imaging and MR spectroscopic data with histologic grade. Radiology 2012; 264:88–96. [CrossRef]

28. Zhong L, Chen JJ, Chen J, et al. Nonalcoholic fatty liver disease: quantitative assessment of liver fat content by computed tomography, magnetic resonance imaging and proton magnetic resonance spectroscopy. J Dig Dis 2009; 10:315–320. [CrossRef]

29. Choji T. Evaluation of fatty liver changes and fatty degeneration in liver tumors by 1H-MRS. Nihon Igaku Hoshasen Gakkai Zasshi 1993; 53:1408–1414.

30. Hamilton G, Middleton MS, Bydder M, et al. Effect of PRESS and STEAM sequences on magnetic resonance spectroscopic liver fat quantification. J Magn Reson Imaging 2009; 30:145–152. [CrossRef]

31. Chabanova E, Bille DS, Thisted E, Holm JC, Thomsen HS. MR spectroscopy of liver in overweight children and adolescents: Investigation of H-1 T-2 relaxation times at 3 T. Eur J Radiol 2012; 81:811–814. [CrossRef]

32. Murayama H, Ikemoto M, Hamaoki M. Ornithine carbamyltransferase is a sensitive marker for alcohol-induced liver injury. Clin Chim Acta 2009; 401:100–104. [CrossRef]

33. Rosenthal P, Haight M. Aminotransferase as a prognostic index in infants with liver disease. Clin Chem 1990; 36:346–348.

34. Sorbi D, Boynton J, Lindor KD. The ratio of aspartate amino-transferase to alanine aminotransferase: Potential value in differentiating non- alcoholic steatohepatitis from alcoholic liver disease. Am J Gastroenterol 1999; 94:1018–1022. [CrossRef]